Open access • Journal Article • DOI:10.1115/1.2931499

Uncertainty Analysis in MCP-Based Wind Resource Assessment and Energy Production Estimation — Source link

Matthew A. Lackner, A. L. Rogers, James F. Manwell

Institutions: University of Massachusetts Amherst

Published on: 01 Aug 2008 - Journal of Solar Energy Engineering-transactions of The Asme (American Society of Mechanical Engineers)

Topics: Wind resource assessment, Uncertainty analysis, Sensitivity analysis, Wind power and Wind speed

August, 2008

Uncertainty Analysis in MCP-Based Wind Resource Assessment and Energy Production Estimation

Matthew Lackner, *University of Massachusetts - Amherst*
Anthony L. Rogers
James F. Manwell

Uncertainty Analysis in MCP-Based Wind Resource Assessment and Energy Production Estimation

Matthew A. Lackner[1]
Ph.D. Student

Anthony L. Rogers
Senior Research Fellow

James F. Manwell
Professor of Mechanical and Industrial Engineering

Renewable Energy Research Laboratory,
University of Massachusetts,
Amherst, MA, 01003

This paper presents a mathematical framework to properly account for uncertainty in wind resource assessment and wind energy production estimation. A meteorological tower based wind measurement campaign is considered exclusively, in which measure-correlate-predict is used to estimate the long-term wind resource. The evaluation of a wind resource and the subsequent estimation of the annual energy production (AEP) is a highly uncertain process. Uncertainty arises at all points in the process, from measuring the wind speed to the uncertainty in a power curve. A proper assessment of uncertainty is critical for judging the feasibility and risk of a potential wind energy development. The approach in this paper provides a framework for an accurate and objective accounting of uncertainty and, therefore, better decision making when assessing a potential wind energy site. It does not investigate the values of individual uncertainty sources. Three major aspects of site assessment uncertainty are presented here. First, a method is presented for combining uncertainty that arises in assessing the wind resource. Second, methods for handling uncertainty sources in wind turbine power output and energy losses are presented. Third, a new method for estimating the overall AEP uncertainty when using a Weibull distribution is presented. While it is commonly assumed that the uncertainty in the wind resource should be scaled by a factor between 2 and 3 to yield the uncertainty in the AEP, this work demonstrates that this assumption is an oversimplification and also presents a closed form solution for the sensitivity factors of the Weibull parameters.
[DOI: 10.1115/1.2931499]

1 Introduction

Wind energy site assessment gauges the potential for a site to produce energy from wind turbines. When wind energy development is under consideration, a site assessment is undertaken. Specifically, it is the process of evaluating the wind resource at a potential wind turbine or wind farm location, then estimating the energy production of the proposed project. The wind resource at a site directly affects the amount of energy that a wind turbine can extract and, therefore, the success of the venture. The wind resource is primarily quantified by the mean wind speed at the site although the turbulence intensity, probability distribution of the wind speed, and prevailing wind direction are also important factors. Once the wind resource is assessed at a site, the expected annual energy production (AEP) of a selected wind turbine is calculated. This calculation combines the expected wind resource with the wind turbine(s) power curve and the expected energy losses in order to estimate how much energy the wind turbine(s) will actually produce at the site. The AEP ultimately helps determine the profitability of the undertaking.

The precision of the wind resource assessment and AEP calculation must also be determined when evaluating a potential site. Wind resource evaluation is an uncertain process, and a large number of factors ranging from wind speed measurement errors to the inherent physical variations in the wind contribute to this uncertainty [1]. These various individual sources of error must all be accounted for in order to provide an estimate of the total uncertainty of the wind resource. Furthermore, power curves and energy loss terms are uncertain as well [2]. When the wind resource, power curve, and energy losses are combined to estimate AEP, uncertainties from all the factors contribute to an overall AEP uncertainty. This uncertainty is critical in estimating the risk associated with the potential venture.

The goal of this paper is to present a logical and rigorous approach for handling uncertainty in the site assessment process. Specifically, it considers the site assessment process in which meteorological towers (met towers) equipped with cup anemometry and vanes are the primary method for evaluating the wind resource, which is the most common method in the US, and measure-correlate-predict (MCP) is used to estimate the long-term wind resource [3,4]. This paper also assumes that measured data are used to create a shear model (i.e., numerical models for shear extrapolation are not considered). Alternative methods for site assessment are not considered. The new methods for uncertainty analysis presented in this paper are in contrast to those recommended in IEC 61400-12, which recommends a bin method [5].

This paper does not present recommended values or estimation tools for various uncertainty sources. Rather, it offers an analytical method for categorizing uncertainty sources in all steps of the site assessment process and then combining the uncertainty sources to yield an overall estimate of the AEP uncertainty. This work aims to provide a framework for site assessment uncertainty analysis founded on a sound mathematical basis.

1.1 Weibull Distribution.

This paper utilizes the Weibull distribution as an approximation of the wind speed distribution. The Weibull distribution is commonly used to model wind speed distributions and often provides a good approximation. It relies on two parameters: the scale factor c and the shape factor k (these

[1]Corresponding author.

Contributed by the Solar Energy Engineering Division of ASME for publication in the JOURNAL OF SOLAR ENERGY ENGINEERING. Manuscript received January 17, 2007; final manuscript received October 4, 2007; published online July 1, 2008. Review conducted by Spyros Voutsinas. Paper presented at the 2007 AIAA Aerospace Sciences Meeting and Exhibit.

two parameters are also related to the mean wind speed according to Eq. (7)). The Weibull probability density function, where U is the wind speed, is as follows [6]:

$$p(U) = (k/c)(U/c)^{k-1} \exp(-(U/c)^k) \quad (1)$$

A statistical model approximation to the wind speed distribution, as opposed to simply using the measured time series or the frequency distribution of the measured data, is useful for several reasons. First, a statistical model allows the shape of the distribution of the wind resource and, therefore, the potential to produce energy from a wind turbine at the site to be quantified by the parameters of the model. In the case of the Weibull distribution, the shape of the distribution of the wind resource is easily summarized by the values of c and k. Second, a statistical model is extremely useful for handling uncertainty both in wind resource assessment and in AEP estimation. Many of the statistical techniques presented in this paper rely on the ability to express the wind speed distribution in a functional form.

On the other hand, a statistical model approximation can introduce error into the process, especially when the model does not provide a good fit to the data. The effect of using a statistical model to represent the wind speed distribution compared to using the actual frequency distribution is investigated and proceeds as follows:

1. 30 different sites, with at least three years of data, are selected.
2. For each site, the mean wind speed and the Weibull parameters are calculated.
3. The actual frequency distribution is also determined, using 0.5 m/s bins.
4. The energy production for a General Electric (GE) 1.5 MW wind turbine is calculated using the actual wind speed frequency distribution, as well as the Rayleigh and Weibull approximations to the wind speed distribution. The Rayliegh distribution is simply the special case of the Weibull distribution with $k=2$. The actual method for calculating energy production is not described here.

The results are determined by comparing the energy production estimates for the two statistical models to the estimate using the actual frequency distribution. The actual frequency distribution is considered the "true" value. The important results are as follows:

- On average, using the Weibull distribution causes a 0.5% overestimation of the energy production compared to using the actual frequency distribution. The error in the estimate has an approximately 1% standard deviation.
- The Rayleigh distribution overestimates the energy production by 3% on average, with a standard deviation of 7%.

Clearly, the Weibull distribution is the superior statistical model, as it results in a lower bias and uncertainty than the Rayleigh distribution. The Weibull distribution is used exclusively in this paper to model the wind speed distribution. The uncertainty associated with the use of the Weibull distribution is small, and so it is neglected in all later analyses.

By using a Weibull distribution to represent the wind speed distribution, the uncertainty in the wind resource can be expressed as uncertainty in the values of c and k. On the other hand, it is often easier to conceptualize and estimate uncertainty in the mean wind speed rather than c. Thus, the uncertainty in the mean wind speed and k is determined first, and then the uncertainty in c is calculated from these values.

2 Brief Review of Error Types and Measurement Uncertainty Analysis

All measurements, no matter how carefully done, are subject to errors, which results in a measured value differing from the true value. The size of the error is unknown, and so all measurements are subject to some uncertainty. In this paper, the term "uncertainty" is used as a general measure of the size of the error. The error in a measurement is comprised of two components: the random error and the systematic error [7].

2.1 Random Error and Uncertainty. Random error is produced by variability in the quantity being measured or in the measurement procedure. For example, when measuring the duration of an event using a stopwatch, random error may arise when multiple measurements are made. The reaction time of the stopwatch operator can vary, causing each measurement to differ. The standard deviation of the measurements is a measure of the uncertainty of a single measurement due to random error. These errors are usually assumed to have normal distributions about the true value.

Often, the mean of the measurements is the quantity of interest. The uncertainty of the mean of the measurements, $\delta\bar{x}$, is equal to the standard deviation of the measurements, σ_x, divided by the square root of the number of measurements N, assuming that the measurements are independent. This relation is shown below [8]:

$$\delta\bar{x} = \sigma_x/\sqrt{N} \quad (2)$$

The uncertainty in the estimate of the mean decreases as the number of measurements increases. Furthermore, this uncertainty is normally distributed for a large N, even if the distribution of the measurements is not normal. The sources of random error are categorized as Type A uncertainty.

2.2 Systematic Error and Unknown Bias Uncertainty. Systematic errors, or biases, are constant over a set of identical measurements [8]. These errors are often due to an error in a calibration constant. An example of a systematic error is a stopwatch that runs slowly. Any measure of the duration of an event with that stopwatch results in a value that is smaller than the true value. Systematic errors cannot be revealed by repeated measurements because they are constant over the set of measurements, assuming that the same instruments are used.

Whenever a measurement is performed, effort should be made to identify the systematic errors and to either remove the source of the errors or to adjust the measurements by the value of the bias. An estimate of the bias of an instrument often requires a comparison to an unbiased instrument or a comparison to measurements from multiple instruments.

The issue is complicated when the bias in a measurement is unknown. However, the bias, while unknown, is constant across every measurement, and so it does not behave like a random error, which varies with each measurement and so can be calculated from the measured data. The uncertainty due to unknown systematic errors is typically estimated based on experience [1]. It has been noted that unknown bias uncertainty can be characterized by a normal distribution, and so the standard deviation is the measurement of the uncertainty [1,5]. In some cases, unknown bias uncertainty is more easily characterized by an uncertainty limit. That is, the estimated distribution is rectangular, with values existing over some range, $\pm R$, with a probability of 1. In these cases, the uncertainty limits can be converted to an equivalent standard deviation. The standard uncertainty δx is equal to R divided by the square root of 3, shown below [5]:

$$\delta x = R/\sqrt{3} \quad (3)$$

The standard deviation of the unknown bias can be measured if multiple instruments are used simultaneously. However, when only a single instrument is used, then the uncertainty has to be approximated. The uncertainty due to unknown bias is categorized as Type B uncertainty.

2.3 Combination of Uncertainties. This paper assumes that all Type A and Type B uncertainties are independent and normally distributed [1,8]. Uncertainties are characterized by the fractional standard uncertainty. The fractional standard uncertainty is the uncertainty of a parameter divided by the absolute value of the

expected value of the parameter. In contrast, the absolute standard uncertainty of a quantity is simply the uncertainty of the parameter, and so it has units. Throughout this paper, a superscript * is used to denote absolute uncertainties. Fractional uncertainties do not have a * superscript.

When multiple uncertain quantities are used to calculate some parameter, the uncertainties in the component quantities combine to yield a total uncertainty in the parameter. For a parameter f, which is a function of several variables, $f=f(x_1,\ldots,x_n)$, the uncertainties of the variables, $\delta x_1^*,\ldots,\delta x_n^*$, are combined to yield an overall uncertainty, δf^*. δf^* is calculated using Eq. (4) as long as the uncertainties are independent,

$$\delta f^* = \sqrt{\left(\frac{\partial f}{\partial x_1}\delta x_1^*\right)^2 + \cdots + \left(\frac{\partial f}{\partial x_n}\delta x_n^*\right)^2} \tag{4}$$

Equation (4) is the standard method for combining independent uncertainties [8]. It can be nondimensionalized so that the uncertainties are expressed as fractional uncertainties. The nondimensional form of Eq. (4) is shown in Eq. (5). The partial derivatives and the fractions, which multiply the fractional uncertainties, are referred to as "sensitivity factors" since they measure how sensitive changes in f are to changes in the variables. The sensitivity factors may be positive or negative in order to indicate if a change in the individual variable causes an increase or a decrease in f. The sign is not particularly important though since the terms are then squared. The sensitivity factors are also nondimensional. As an example, anytime f has a linear dependence on a variable, the sensitivity factor for that variable is 1. When all of the sensitivity factors are 1, then Eq. (5) reduces to a simple "root-sum-square" (RSS) technique,

$$\delta f = \sqrt{\left(\frac{\partial f}{\partial x_1}\frac{x_1}{f}\delta x_1\right)^2 + \cdots + \left(\frac{\partial f}{\partial x_n}\frac{x_n}{f}\delta x_n\right)^2} \tag{5}$$

Type A and Type B uncertainties can be combined together using Eq. (5) as long as they are each expressed using the standard deviation as a measure of uncertainty. It must be emphasized that there is no definitive method for combining Type A errors and Type B errors. This method is likely the best available option, assuming that the individual uncertainty sources are independent [1,8]. Also, by the central limit theorem, the distribution of the total uncertainty tends toward a normal distribution, regardless of the distribution of the individual sources of uncertainty. In this paper, all sources of uncertainty are assumed to be normally distributed, so the distribution of the total uncertainty is also normal.

3 Wind Resource Uncertainty

Wind resource evaluation consists of using measured wind speed data to estimate the long-term hub height wind resource at the turbine locations. When the Weibull distribution is used to characterize the wind resource, the goal of wind resource assessment is to estimate the long-term hub height values of the Weibull parameters, $c_{\mathrm{LT\_hub}}$ and $k_{\mathrm{LT\_hub}}$.

This section describes four categories of uncertainty sources that arise in wind resource assessment. Within each category of uncertainty, there are several individual uncertainty sources. A brief description of each category, including the individual component uncertainty sources, is provided. Again, methods for estimating or calculating these uncertainty sources are not discussed. Rather, this section intends to categorize the uncertainty sources and describe a method to combine them once the actual values have been estimated. However, for completeness, numerous references that explore each of these uncertainty sources in detail are provided below.

There are a total of 14 individual component uncertainty sources identified in this paper. they contribute to the wind resource uncertainty, but this list certainty is not necessarily exhaustive and other uncertainty sources are possible. These uncertainty sources are assumed to be independent. The wind resource uncertainty sources can be expressed as uncertainty in the values of the mean wind speed and k, and then the uncertainty of c can be calculated afterward.

3.1 Categories of Wind Resource Uncertainty. The causes of uncertainty in wind resource assessment can be subdivided into four categories: wind speed measurement uncertainty, long-term resource estimation uncertainty, wind resource variability uncertainty, and site assessment uncertainty. These four categories are labeled with subscripts M, LT, V, and SA. Each category is now discussed briefly, and the component uncertainty sources within each category are listed.

3.1.1 Wind Speed Measurement Uncertainty. The wind speed at a site is usually measured by taking 10 min averages of the wind speed, sampled at approximately 1 Hz. Wind data at a site are then presented as a time series of these 10 min averages. Several factors can contribute to errors in the measurement of the wind speed. These factors fall into the category of wind speed measurement uncertainty. They are as follows:

1. anemometer uncertainty I: calibration uncertainty [9,10]
2. anemometer uncertainty II: dynamic overspeeding [11,12]
3. anemometer uncertainty III: vertical flow effects [2]
4. anemometer uncertainty IV: vertical turbulence effects [11–13]
5. tower effects [14]
6. boom and mounting effects [15]
7. data processing accuracy

3.1.2 Long-Term Resource Estimation Uncertainty. While wind resource measurement typically lasts for one year, the measured resource during this particular year may not be representative of the actual long-term resource at the site. Twenty to thirty years is sometimes assumed to be a long enough time period to characterize the long-term wind resource [16,17]. Since a 20-year measurement campaign is far too long for practical purposes, the long-term resource must be estimated from the measured data.

One common method for estimating the long-term wind resource utilizes the measured data, along with long-term data from a nearby site (the "reference site"), in a process called MCP [18,19]. While there are other methods as well, MCP is considered exclusively in this paper. The long-term mean wind speed and Weibull parameters estimated from MCP can be labeled as $\bar{U}_{\mathrm{LT}}$, c_{LT}, and k_{LT}, MCP introduces uncertainty into the estimate of the long-term resource at the site. In general, longer measurement periods and longer reference site data sets result in less uncertainty in the MCP process [20].

An additional uncertainty arises when Weibull parameters are fited to the output of the MCP step. Since the output data of MCP is not a perfect Weibull distribution, different estimation methods yield different values of the Weibull parameters. The result is an additional uncertainty in the values of c_{LT}, and k_{LT}. There are several methods of estimating the Weibull parameters from a wind speed time series. These methods include empirical methods, method of moments, maximum likelihood estimates, least square linear regression, and chi-squared methods [6]. While the uncertainty in the estimation of c_{LT} is negligibly small, there can be a significant variation in k_{LT}.

Finally, global climate change may also cause uncertainty in the estimate as the actual climate at a site may change in the future [21].

The three uncertainty sources that arise in a long-term resource estimation are as follows

1. MCP correlation uncertainty [20]
2. Weibull parameter estimation uncertainty
3. changes in the long-term average [21]

3.1.3 Wind Resource Variability Uncertainty. The wind resource varies from year to year, and these interannual variations

can cause uncertainty in two ways [16,17]. First, the reference site data used in the MCP step to estimate the long-term parameters might not, in fact, be representative of the true long-term resource. Since random error decreases as the number of samples increases, the longer the reference site data set used in the MCP step to estimate the long-term parameters, the less uncertainty there is in these estimates. Second, interannual variability can cause the actual wind resource that occurs over the lifetime of a turbine to be different from the true long-term wind resource, which produces additional uncertainty. These two uncertainty sources are independent of the issue of global climate change contributing to changes in the long-term average, which is discussed above. Instead, these two uncertainty sources are related to sampling variability in the long-term wind resource at the site, and not to the large scale changes in the climate itself. These two uncertainties are therefore type A uncertainties, and they are

1. reference site inter-annual variability
2. inter-annual variability over a turbine lifetime

3.1.4 Site Assessment Uncertainty. Wind speed measurements usually take place at heights significantly lower than the hub height of a typical modern wind turbine. Because wind speeds typically increase with height, a wind shear model is often used to extrapolate the estimated long-term wind resource to the hub height [22]. The wind shear model is usually created using the measured wind speed data [23].

The tower used to measure the wind speed is often not at the exact location of the wind turbine(s). Topographic effects can cause the wind speeds at separate locations at a site to differ, and so flow models can be used to estimate the wind resource at each turbine location [24]. A variety of different approaches to flow modeling are possible, and each introduces some uncertainty.

Uncertainty arises when modeling both the wind shear and the topographic effects on wind speed at a site and, therefore, when estimating the long-term, hub height mean wind speed and Weibull parameters at the probable turbine location, $\bar{U}_{\mathrm{LT\_hub}}$, $c_{\mathrm{LT\_hub}}$, and $k_{\mathrm{LT\_hub}}$. The models may not, in fact, be accurate, and so error can be introduced into these transformations. The two factors contributing to this uncertainty are

1. topographic model uncertainty [24]
2. wind shear model uncertainty [22,23]

3.2 Estimation of the Wind Resource. Once the wind speed measurements at the site are completed, an estimate can be made of the long-term hub height wind resource and the associated uncertainty in this estimate. This section describes a process for estimating the long-term hub height mean wind speed and Weibull parameters, $\bar{U}_{\mathrm{LT\_hub}}$, $c_{\mathrm{LT\_hub}}$, and $k_{\mathrm{LT\_hub}}$. The next section discusses the associated uncertainty. The process for estimating the wind resource informs the process for estimating the uncertainty. The steps used to determine the long-term hub height wind resource are listed below.

1. Correct for any known bias in the measured wind speed. The anemometer vertical sensitivity, the anemometer overspeeding, the anemometer vertical turbulence effects, and the tower effects may introduce a bias into the measurement of the wind speed. The measured wind speed data should be scaled to remove these biases.
2. Use the measured wind speed data to determine the appropriate shear parameter. If the power law is used, then solve for α. If the log law is used, then solve for z_0 (a stability correction may also be necessary for the log law).
3. Use the measured wind speed data and data from a long-term reference site in a MCP algorithm. The outputs of the MCP algorithm are estimates of the long-term mean wind speed and long-term Weibull shape factor at the measurement height and location, $\bar{U}_{\mathrm{LT}}$ and k_{LT}. Any of several methods for estimating k_{LT} from time series data can be used, including empirical methods or maximum likelihood methods.
4. Apply the chosen shear model to $\bar{U}_{\mathrm{LT}}$, the output of the MCP step. For example, if one utilizes the power law, then after determining α in step 2, Eq. (6) is used to calculate $\bar{U}_{\mathrm{LT\_hub}}$. h_3 is the hub height, and h_2 is the highest measurement height.

$$\bar{U}_{\mathrm{LT\_hub}} = \bar{U}_{\mathrm{LT}}(h_3/h_2)^{\alpha} \tag{6}$$

5. Apply a shear model to extrapolate the estimated long-term shape factor k_{LT} to the hub height. k typically increases with height, although generally much less strongly than the mean wind speed. While various models exist for extrapolating k with height, the predictions from these models are highly variable, with little predictive value [25,26]. Furthermore, for common measurement heights ($\sim$50 m) and modern turbine hub heights ($\sim$80 m), the models predict small increases in k on the order of 5% [26]. To date, no shear model for k is recommended here, and one can also either assume that k remains constant with height or apply a small correction factor on the order of 5–10%, which is typical. Future work may investigate alternative models for k extrapolation.
6. Apply a topographic correction, if necessary, to determine the hub height wind resource at each of the turbine locations [24].
7. Correct for any known bias in the shear extrapolation and topographic correction. These processes can introduce bias, and so the estimated value of $\bar{U}_{\mathrm{LT\_hub}}$ and $k_{\mathrm{LT\_hub}}$ should be scaled to remove these biases [22,24].
8. Calculate the value of $c_{\mathrm{LT\_hub}}$ at each turbine location from the values of $\bar{U}_{\mathrm{LT\_hub}}$ and $k_{\mathrm{LT\_hub}}$ at each turbine location. This can be done using Eq. (7), where Γ is the gamma function [6]

$$c_{\mathrm{LT\_hub}} = \bar{U}_{\mathrm{LT\_hub}}/\Gamma(1 + 1/k_{\mathrm{LT\_hub}}) \tag{7}$$

It must be emphasized that because of topographic corrections, the values of $\bar{U}_{\mathrm{LT\_hub}}$, $c_{\mathrm{LT\_hub}}$, and $k_{\mathrm{LT\_hub}}$ are likely different for each turbine location.

3.3 Wind Resource Uncertainty. Once the long-term wind resource is determined, the uncertainty of the long-term wind resource is then estimated. The estimates of the individual uncertainty values for the mean wind speed are labeled δU_i, and for the shape factor they are labeled δk_i. The steps to determine the uncertainty are as follows:

1. Use Eq. (5) to combine the uncertainty values within each category of uncertainty for the mean wind speed. This is shown in Eq. (8). The subscripts M, LT, V, and SA correspond to uncertainty in the four categories of uncertainty. Within each category of uncertainty, the sensitivity factors are equal to 1 because each uncertainty source contributes equally and linearly to the overall uncertainty of the category, and so a simple RSS method can be used.

$$\text{I: } \delta U_{\mathrm{M}} = \sqrt{(\delta U_1)^2 + (\delta U_2)^2 + (\delta U_3)^2 + (\delta U_4) + (\delta U_5)^2 + (\delta U_6)^2 + (\delta U_7)^2}$$

$$\text{II: } \delta U_{\mathrm{LT}} = \sqrt{(\delta U_8)^2 + (\delta U_9)^2 + (\delta U_{10})^2}$$

$$\text{III: } \delta U_{\mathrm{V}} = \sqrt{(\delta U_{11})^2 + (\delta U_{12})^2}$$

$$\text{IV: } \delta U_{\mathrm{SA}} = \sqrt{(\delta U_{13})^2 + (\delta U_{14})^2} \tag{8}$$

2. The general equations to determine δU is derived from Eq. (5). The result is shown in Eq. (9). The sensitivity factors for the mean wind speed for each category of uncertainty are $\mathrm{SF}_{U,\mathrm{M}}$, $\mathrm{SF}_{U,\mathrm{LT}}$, $\mathrm{SF}_{U,\mathrm{V}}$, and $\mathrm{SF}_{U,\mathrm{SA}}$,

$$\delta U = \sqrt{(\mathrm{SF}_{U,\mathrm{M}}\delta U_{\mathrm{M}})^2 + (\mathrm{SF}_{U,\mathrm{LT}}\delta U_{\mathrm{LT}})^2 + (\mathrm{SF}_{U,\mathrm{V}}\delta U_{\mathrm{V}})^2 + (\mathrm{SF}_{U,\mathrm{SA}}\delta U_{\mathrm{SA}})^2} \quad (9)$$

3. Determine the sensitivity factors for each category of uncertainty. The sensitivity factor for the wind resource variability uncertainty and the site assessment uncertainty are both equal to 1 since they contribute linearly to the overall uncertainty. Thus, $\mathrm{SF}_{U,\mathrm{V}}=\mathrm{SF}_{U,\mathrm{SA}}=1$.

   If a linear model is used in the MCP step, then the sensitivity factor for the long-term resource estimation for the mean wind speed, $\mathrm{SF}_{U,\mathrm{LT}}$, is also equal to 1. The Renewable Energy Research Laboratory (RERL) uses a linear MCP model, dubbed the "variance ratio" method, which has been shown to perform well relative to other models [27]. From an uncertainty perspective, using a linear model simplifies the calculation of the overall wind resource uncertainty.

   The sensitivity factor for the measurement uncertainty, $\mathrm{SF}_{U,\mathrm{M}}$, is not equal to 1, because the measured wind speed is used to calculate the shear parameter and the shear parameter is then used to estimate $\bar{U}_{\mathrm{LT\_hub}}$. The result is that error in the measurement of the wind speed causes error in the shear parameter calculation, which then causes additional error in the estimate of $\bar{U}_{\mathrm{LT\_hub}}$ [28]. Thus, the contribution of measurement uncertainty to the total uncertainty is magnified due to shear extrapolation, and so the sensitivity factor for the measurement uncertainty is greater than 1. It is important to emphasize that this effect is not due to any error in the wind shear model. Rather, it is a mathematical byproduct of using uncertain data to determine an extrapolation parameter.

   $\mathrm{SF}_{U,\mathrm{M}}$ can be calculated as follows: h_1, h_2, and h_3 are the heights of the lower measurement anemometer, the higher measurement anemometer, and the hub height, respectively. $\bar{U}_{\mathrm{M1}}$ and $\bar{U}_{\mathrm{M2}}$ are the measured mean wind speeds at the lower and upper anemometers, respectively. When the power law is used, the measured data can be used to calculate the shear parameter α using

$$\alpha = \ln(\bar{U}_{\mathrm{M2}}/\bar{U}_{\mathrm{M1}})/\ln(h_2/h_1) \quad (10)$$

   The predicted mean wind speed $\bar{U}_{\mathrm{hub}}$ at height h_3 can then be calculated using

$$\bar{U}_{\mathrm{hub}} = \bar{U}_{\mathrm{M2}}(h_3/h_2)^{\ln(\bar{U}_{\mathrm{M2}}/\bar{U}_{\mathrm{M1}})/\ln(h_2/h_1)} \quad (11)$$

   If it is assumed that the uncertainties in the mean wind speeds are independent and normally distributed and if there is no uncertainty in the three heights, then the uncertainties can be related using

$$\delta\bar{U}^*_{\mathrm{hub}} = \sqrt{\left(\frac{\partial\bar{U}_{\mathrm{hub}}}{\partial\bar{U}_{\mathrm{M1}}}\delta\bar{U}^*_{\mathrm{M1}}\right)^2 + \left(\frac{\partial\bar{U}_{\mathrm{hub}}}{\partial\bar{U}_{\mathrm{M2}}}\delta\bar{U}^*_{\mathrm{M2}}\right)^2} \quad (12)$$

   Next, it is assumed that the fractional standard uncertainty of $\bar{U}_{\mathrm{M1}}$ and $\bar{U}_{\mathrm{M2}}$ ($\delta\bar{U}_{\mathrm{M1}}$ and $\delta\bar{U}_{\mathrm{M2}}$) are both equal to the fractional standard measurement uncertainty δU_{M}, as shown in Eq. (13). That is, it is assumed that the measurement uncertainties at both heights are identical,

$$\delta U_{\mathrm{M}} = \delta\bar{U}_{\mathrm{M1}} = \delta\bar{U}_{\mathrm{M2}} = \delta\bar{U}^*_{\mathrm{M1}}/\bar{U}_{\mathrm{M1}} = \delta\bar{U}^*_{\mathrm{M2}}/\bar{U}_{\mathrm{M2}} \quad (13)$$

   Finally, after substituting Eq. (13) into Eq. (12) and after some algebraic manipulation, the ratio of the fractional uncertainty in the predicted mean wind at height h_3, $\delta\bar{U}_{\mathrm{hub}}$, to the fractional standard measurement uncertainty δU_{M} can be written using Eq. (14). This ratio is also equal to $\mathrm{SF}_{U,\mathrm{M}}$,

$$\mathrm{SF}_{U,\mathrm{M}} = \frac{\delta\bar{U}_{\mathrm{hub}}}{\delta U_{\mathrm{M}}} = \sqrt{\left(\frac{\partial\bar{U}_{\mathrm{hub}}}{\partial\bar{U}_{\mathrm{M1}}}\frac{\bar{U}_{\mathrm{M1}}}{\bar{U}_{\mathrm{M2}}}\right)^2 + \left(\frac{\partial\bar{U}_{\mathrm{hub}}}{\partial\bar{U}_{\mathrm{M2}}}\right)^2}\cdot\left(\frac{\bar{U}_{\mathrm{M2}}}{\bar{U}_{\mathrm{hub}}}\right) \quad (14)$$

   The partial derivatives and the ratios $\bar{U}_{\mathrm{M1}}/\bar{U}_{\mathrm{M2}}$ and $\bar{U}_{\mathrm{M2}}/\bar{U}_{\mathrm{hub}}$ can be calculated using Eq. (11). When these calculations are substituted into Eq. (14), $\mathrm{SF}_{U,\mathrm{M}}$ can be written as an analytic function of only the three measurement heights. The final result for $\mathrm{SF}_{U,\mathrm{M}}$ is shown in

$$\mathrm{SF}_{U,\mathrm{M}} = \sqrt{\frac{2\left(\ln\left(\frac{h_3}{h_2}\right)\right)^2 + \left(\ln\left(\frac{h_2}{h_1}\right)\right)^2 + 2\ln\left(\frac{h_2}{h_1}\right)\ln\left(\frac{h_3}{h_2}\right)}{\left(\ln\left(\frac{h_2}{h_1}\right)\right)^2}} \quad (15)$$

   As an example, for a met tower with measurement heights of 35 m and 50 m, and a turbine hub height of 80 m, $\mathrm{SF}_{U,\mathrm{M}}=2.7$. The result is that the measurement uncertainty can contribute significantly more to the overall wind resource uncertainty than its actual value would indicate, due to this shear extrapolation effect.

4. Calculate the overall uncertainty in the long-term hub height mean wind speed δU. This is accomplished using Eq. (9). Because $\mathrm{SF}_{U,\mathrm{LT}}=\mathrm{SF}_{U,\mathrm{V}}=\mathrm{SF}_{U,\mathrm{SA}}=1$, the equation for δU can be written as

$$\delta U = \sqrt{(\mathrm{SF}_{U,\mathrm{M}}\delta U_{\mathrm{M}})^2 + (\delta U_{\mathrm{LT}})^2 + (\delta U_V)^2 + (\delta U_{\mathrm{SA}})^2} \quad (16)$$

5. Determine δk. The RSS method can be used to combine the uncertainty values within each category of uncertainty for k, as shown in

$$\text{I: } \delta k_{\mathrm{M}} = \sqrt{(\delta k_1)^2 + (\delta k_2)^2 + (\delta k_3)^2 + (\delta k_4) + (\delta k_5)^2 + (\delta k_6)^2 + (\delta k_7)^2}$$

$$\text{II: } \delta k_{\mathrm{LT}} = \sqrt{(\delta k_8)^2 + (\delta k_9)^2 + (\delta k_{10})^2}$$

$$\text{III: } \delta k_{\mathrm{V}} = \sqrt{(\delta k_{11})^2 + (\delta k_{12})^2}$$

$$\text{IV: } \delta k_{SA} = \sqrt{(\delta k_{13})^2 + (\delta k_{14})^2} \quad (17)$$

6. The general equation for δk is shown in Eq. (18). The sensitivity factors for k for each category of uncertainty are $\mathrm{SF}_{k,\mathrm{M}}\mathrm{SF}_{k,\mathrm{LT}}\mathrm{SF}_{k,\mathrm{V}}$, and $\mathrm{SF}_{k,\mathrm{SA}}$,

$$\delta k = \sqrt{(\mathrm{SF}_{k,\mathrm{M}}\delta k_{\mathrm{M}})^2 + (\mathrm{SF}_{k,\mathrm{LT}}\delta k_{\mathrm{LT}})^2 + (\mathrm{SF}_{k,V}\delta k_V)^2 + (\mathrm{SF}_{k,\mathrm{SA}}\cdot\delta k_{\mathrm{SA}})^2} \quad (18)$$

7. Determine the sensitivity factors for each category of uncertainty for k. As is the case for the mean wind speed, $\mathrm{SF}_{k,\mathrm{LT}}=\mathrm{SF}_{k,\mathrm{V}}=\mathrm{SF}_{k,\mathrm{SA}}=1$, as long as a linear MCP model is used. The value of $\mathrm{SF}_{k,\mathrm{M}}$ depends on the method used to extrapolate k. If k is assumed to be constant with height, or if a simple scale factor is utilized, then $\mathrm{SF}_{k,\mathrm{M}}$ is simply 1. However, if measured data are used to calculate a shear parameter for a shear model for k, then $\mathrm{SF}_{k,\mathrm{M}}$ is larger than 1 since uncertain data are used to calculate the shear model parameter. A similar analysis as that performed in step 3 above would then be necessary to determine $\mathrm{SF}_{k,\mathrm{M}}$.
8. δc can then be calculated based on δU and δk using Eq. (7). The general equation for δc is shown in

$$\delta c = \sqrt{(\mathrm{SF}_{c,\mathrm{U}}\delta U)^2 + (\mathrm{SF}_{c,k}\delta k)^2} \quad (19)$$

$\mathrm{SF}_{c,\mathrm{U}}$ is simply equal to 1 due to the linear dependence shown in Eq. (7). The formula for $\mathrm{SF}_{c,k}$ is shown below in Eq. (20), where ψ is the psi function,

$$\mathrm{SF}_{c,k} = \frac{\partial c}{\partial k}\frac{k}{c} = \psi(1 + 1/k)/k \tag{20}$$

In general, other sources of uncertainty are possible in the site assessment process. Furthermore, alternative methods of performing a site assessment are also viable approaches; for instance, mesoscale and microscale modeling can be used instead of MCP [18]. These alternative site assessment methods necessitate modification to the uncertainty analysis approach outlined above. However, many of the above techniques are applicable.

4 Wind Turbine Power Production and Uncertainty

Like the wind resource, the determination of the power curve and power production of a wind turbine is also potentially subject to error, which then causes uncertainty in the estimate of AEP.

4.1 Wind Turbine Power Production Uncertainty Sources. Three sources of power production uncertainty are identified. A detailed discussion of the causes and sizes of these uncertainty sources is not presented. Rather, the three uncertainty sources are listed and a brief discussion is provided. For completeness, references to more detailed descriptions of these uncertainty sources and their values are provided. The three sources of power production uncertainty are labeled δP_1, δP_2, and δP_3. They are

1. wind turbine specimen variation [1,29]
2. wind turbine power curve uncertainty [1,5,29]
3. air density uncertainty

Wind turbine specimen variation is caused by variations of individual turbine power curves within a particular model from the "reference" power curve quoted by the manufacturer [1,29]. These variations are likely due to manufacturing variations.

The power curve uncertainty is typically significantly larger than the other two uncertainties. When power curves for wind turbines are measured by the manufacturer, several factors contribute to the uncertainty in this "measured power curve." The primary factor is uncertainty in the wind speed to which the turbine responds because the uncertainty in the actual power being produced is quite small. While the wind speed at the hub height is known to a fairly high accuracy, the effects of turbulence and shear across the rotor face are not taken into account, and consequently the mean wind speed averaged over the rotor face is uncertain [1,5,29].

This issue is exacerbated when a turbine is placed at a particular site because the power curve of a wind turbine is site dependent and not solely a function of the hub height wind speed. The turbulence, air density, and shear characteristics of a site affect the power curve of a turbine, with the result that a turbine at a specific site could produce either more or less power than the power curve indicates at a given wind speed. The measured power curve specifically corresponds to a site that meets the IEC 61400-12 standards, which require a flat site with very low turbulence [5]. Thus, a site-specific power curve is needed to estimate energy production at a site, especially when the terrain is complex. The manufacturer generally determines this site-specific power curve.

Air density uncertainty is caused by seasonal variations in the air density over the course of a year, if the average air density at the site is used to adjust the power curve. This tends to be a small effect relative to the other two, even at sites with large seasonal variations in air density.

4.2 Wind Turbine Power Production Uncertainty. The overall power production uncertainty can be calculated using the general equation given in Eq. (5). The three uncertainty sources are independent, and the sensitivity factor for each is 1. Thus, the overall power production uncertainty δP is shown in

$$\delta P = \sqrt{(\delta P_1)^2 + (\delta P_2)^2 + (\delta P_3)^2} \tag{21}$$

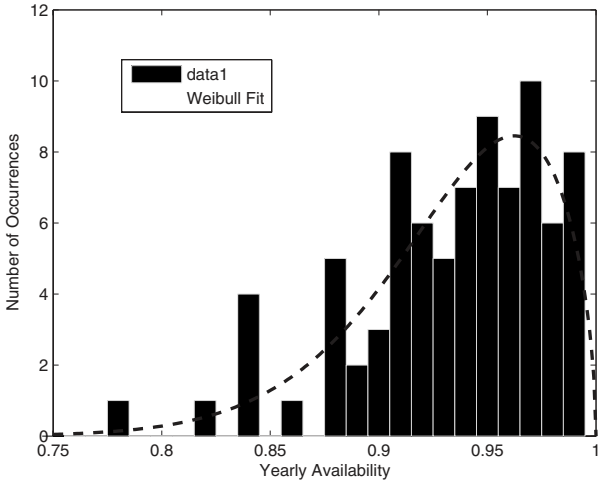

Fig. 1 Empirical availability data and Weibull fit

5 Wind Turbine Energy Production Losses and Uncertainty

This section describes the factors that contribute to uncertainty in the estimate of energy losses. These factors are distinct from those described in the previous section, which are related to uncertainty in the instantaneous power output and are referred to as "energy loss factors" (ELFs).

5.1 Energy Loss Factors. Three ELFs have been identified. Although other losses are also possible, they are not considered here. Each of these factors reduces the energy production of a wind turbine or wind farm. They are

1. availability losses [30]
2. fouling (dirt) and icing losses [31,32]
3. array losses [33]

These three ELFs are labeled $\mathrm{ELF}_{\mathrm{av}}$, $\mathrm{ELF}_{\mathrm{foul}}$, and $\mathrm{ELF}_{\mathrm{array}}$. Each ELF is defined as the ratio of the actual energy produced divided by the ideal energy production if there are no losses. Thus, $\mathrm{ELF}_{\mathrm{av}}$ is simply equal to the actual expected energy production of the wind turbine or wind farm, divided by the hypothetical energy production if there is no maintenance of the turbine(s) or down time, whether scheduled or unscheduled. The other two ELFs have equivalent definitions. $\mathrm{ELF}_{\mathrm{array}}$ is typically calculated using a wake model.

The total reduction to the wind turbine or wind farm energy loss is simply the product of the three ELFs. Thus, the overall ELF is shown in Eq. (22). The ELFs are independent, and a normal distribution is assumed for each,

$$\mathrm{ELF} = \mathrm{ELF}_{\mathrm{av}}\mathrm{ELF}_{\mathrm{foul}}\mathrm{ELF}_{\mathrm{array}} \tag{22}$$

5.2 Justification of Normally Distributed Energy Loss Factors. The assumption of a normal distribution must now be justified. The ELFs, by definition, have a range between 0% and 100%. A normal distribution is defined at $[-\infty, \infty]$. This is a clear contradiction because a normally distributed ELF implies the possibility of a value less than zero or greater than 1. Despite this contradiction, normally distributed ELFs are used, and there is a sound mathematical basis for their use.

The yearly availability of a wind farm is not a normally distributed quantity about its expected value. This can be seen clearly in the histogram in Fig. 1. The data in Fig. 1 show the number of occurrences of yearly availability values for 25 different wind farms, with a total of 104 wind farm years of operation. The mean availability is approximately 94%, and the distribution is clearly asymmetrical, with an upper limit of 100%. These data are com-

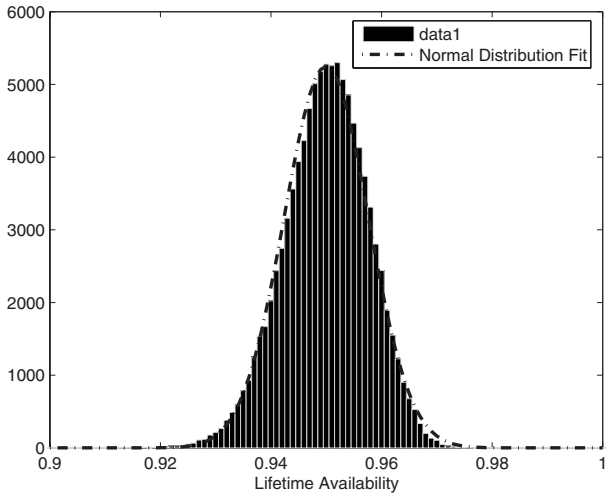

Fig. 2 Distribution of lifetime availability values

piled from a variety of North American wind farms [30].

The data in Fig. 1 can be fitted with a Weibull distribution, for example. The choice of a Weibull distribution is fairly arbitrary although it does provide a good fit to the empirical data. The Weibull approximation to the data is also shown in Fig. 1. The shape factor has a value of $k=1.5$.

The yearly availability is not the quantity used in AEP estimates, however. When estimating AEP, the average availability over the approximately 20-year lifetime of the project is used in the estimate. Thus, the quantity of interest is the lifetime availability of the wind farm or the average of the 20 yearly availability values. The distribution of the lifetime availability can be determined using a Monte Carlo simulation, assuming that the yearly availability in any given year is independent of other years. The simulation proceeds as follows:

1. Twenty values are randomly sampled from a Weibull distribution with an expected value of 0.94 and a $k=1.5$, which is the Weibull fit to the empirical availability data. These 20 values represent a random set of wind farm yearly availability values.
2. These 20-year availability values are averaged to get the lifetime availability.
3. This process is repeated 100,000 times.

The distribution of the lifetime availability values can then be plotted in a histogram. This is shown in Fig. 2. A normal distribution can be fitted to the data and is shown in Fig. 2 as well. The mean is 0.94 and the standard deviation is 0.009.

Thus, while the distribution of yearly availability values can be approximated by a Weibull distribution, the distribution of lifetime availability values is very closely approximated by a normal distribution. This result should not be surprising, and it follows directly from the central limit theorem. This result makes intuitive sense as well. The yearly availability distribution from Fig. 1 indicates that there is approximately a 10% chance of getting an availability value less than 0.90 in a single year. However, the chance of getting availability values less than 0.90 over the lifetime of the project is extremely small, and this is reflected in Fig. 2. Over a 20-year period, it is unlikely that the average availability is much different than the expected value.

This result can be applied to all three ELFs. Like the availability, the yearly distributions of $\mathrm{ELF_{foul}}$ and $\mathrm{ELF_{array}}$ cannot be normally distributed. Instead, they most likely follow a similar asymmetrical distribution, with an upper limit of 1. However, the distribution of the 20-year average once again follows a normal distribution due to the central limit theorem.

There is still the possibility for values greater than 1 when normally distributed ELFs are assumed, and so a contradiction remains. In general, however, the probability of a value greater than 1 is so small that it is completely negligible.

5.3 Energy Loss Factors and Uncertainty. The ELFs are independent and normally distributed, and the overall ELF uncertainty δELF can be calculated using Eq. (5), as long as the individual energy loss factor uncertainties, $\delta\mathrm{ELF_{av}}$, $\delta\mathrm{ELF_{foul}}$, and $\delta\mathrm{ELF_{array}}$, are expressed as fractional standard uncertainties. The sensitivity factor for each ELF is 1 since the overall ELF is simply the product of the three individual ELFs. The resulting equation for δELF is given in

$$\delta\mathrm{ELF} = \sqrt{(\delta\mathrm{ELF_{av}})^2 + (\delta\mathrm{ELF_{foul}})^2 + (\delta\mathrm{ELF_{array}})^2} \tag{23}$$

6 Energy Production and Uncertainty

Once the wind resource at a site has been determined, it is combined with a selected power curve and the ELFs to yield an estimate of the energy production of the wind turbine or wind farm. The uncertainty in the wind resource, the power production, and the ELFs contribute to an overall uncertainty in the energy production. Often, it is more convenient to use the "capacity factor" (CF) as a measure of energy production, which is used exclusively as a measure of energy production for the rest of this section.

This section reviews both one common method for combining the wind resource, power curve, and ELFs to estimate CF and a new method for combining the uncertainties of each of these terms to yield the uncertainty of CF. The methods described in this section can be applied to either a single wind turbine or a wind farm. The total wind farm energy production is simply the sum of the energy productions of each turbine, and the wind farm CF is simply the average of all the wind turbine CFs. The effect of wake losses on individual turbines is encompassed in the $\mathrm{ELF_{array}}$, which is a measure of the total energy loss of the wind farm due to wake losses. Topographic effects are accounted for by using a different value of $c_{\mathrm{LT\_hub}}$ and $k_{\mathrm{LT\_hub}}$ for each wind turbine.

6.1 Capacity Factor Estimation. The capacity factor is a function of the long-term hub height Weibull parameters, which are simply labeled c and k in this section, along with a wind turbine power curve P_W and the overall ELF. In one common approach, the value can be calculated by integrating the product of the wind speed probability distribution and the power curve over all values of wind speed U, multiplying by the overall ELF, and dividing by the rated power. The wind speed probability distribution is the Weibull distribution, given in Eq. (1), with the long-term hub height values of c and k used as the Weibull parameters. This is shown in [6]

$$\mathrm{CF} = \overline{P_W}/P_R = (\mathrm{ELF}/P_R) \cdot \int_0^\infty P_W(U)(k/c)(U/c)^{k-1} \times \exp[-(U/c)^k]dU \tag{24}$$

The integral in Eq. (24) cannot be performed analytically. Instead, it must be approximated numerically. A trapezoid method or Simpson's method can be easily implemented to perform this integral. This formulation is convenient because the entire contribution of the wind resource to CF is condensed in the values of c and k.

6.2 Capacity Factor Uncertainty Estimation. A new method for determining the uncertainty of CF is now presented. The general equation for δCF is given in

$$\delta\mathrm{CF} = \sqrt{\left[\left(\frac{\partial \mathrm{CF}}{\partial c}\frac{c}{\mathrm{CF}}\right)\delta c\right]^2 + \left[\left(\frac{\partial \mathrm{CF}}{\partial k}\frac{k}{\mathrm{CF}}\right)\delta k\right]^2 + \delta P^2 + \delta\mathrm{ELF}^2} \tag{25}$$

This is derived from the general uncertainty formula in Eq. (5). The terms multiplying δc and δk (the partial derivatives and the fractions inside the parentheses) in Eq. (25) are the sensitivity factors for c and k. The sensitivity factors for c and k are labeled $SF_{CF,c}$ and $SF_{CF,k}$, respectively. The sensitivity factors for δP and δELF are 1 since CF has a linear dependence on these quantities.

The calculation of $SF_{CF,c}$ and $SF_{CF,k}$ begins with Eq. (24). The partial derivatives can be taken using the Leibniz integration rule, shown in Eqs. (26) and (27). $p(U)$ is the Weibull probability density function,

$$SF_{CF,c} = \frac{\partial CF}{\partial c}\frac{c}{CF} = \frac{1}{CF}\frac{ELF}{P_R}\int_0^\infty P_W(U)\frac{\partial p(U)}{\partial c}cdU \quad (26)$$

$$SF_{CF,k} = \frac{\partial CF}{\partial k}\frac{k}{CF} = \frac{1}{CF}\frac{ELF}{P_R}\int_0^\infty P_W(U)\frac{\partial p(U)}{\partial k}kdU \quad (27)$$

After the derivatives are taken and some algebraic manipulation is carried out, the sensitivity factors can be written as shown in Eqs. (28) and (29). The integrals cannot be calculated analytically, but once again numerical integration can be used to estimate the sensitivity factors

$$SF_{CF,c} = \frac{1}{CF}\frac{ELF}{P_R}\int_0^\infty P_W(U)k\left(\left(\frac{U}{c}\right)^k - 1\right)p(U)dU \quad (28)$$

$$SF_{CF,k} = \frac{1}{CF}\frac{ELF}{P_R}\int_0^\infty P_W(U)\left(1 + k\ln\left(\frac{U}{c}\right)\left(1 - \left(\frac{U}{c}\right)^k\right)\right)p(U)dU \quad (29)$$

Finally, δCF can be calculated using the general equation given in Eq. (25),

$$\delta CF = \sqrt{(SF_{CF,c}\delta c)^2 + (SF_{CF,k}\delta k)^2 + \delta P^2 + \delta ELF^2} \quad (30)$$

The utility of this new method for estimating the uncertainty of the energy production in the site assessment process rests in the ability to explicitly calculate sensitivity factors using Eqs. (28) and (29) rather than assume values. The method recommended in IEC 61400-12, while equally valid, utilizes a bin method, which may be more cumbersome and less elegant than the method presented here [5]. Furthermore, the values of the sensitivity factors give insight into the contribution of the component uncertainty sources to the overall uncertainty.

6.3 Example Calculation of Capacity Factor and Capacity Factor Uncertainty. An sample calculation helps to clarify the process. The important assumptions and values in the example are given below:

1. The long-term hub height Weibull parameters are $c=9$ m/s and $k=2.5$. This would be considered an excellent site for wind energy development.
2. A GE 1.5 MW wind turbine power curve is used for this example. This power curve is shown in Fig. 3. This is a variable speed, pitch regulated wind turbine.
3. The total energy losses reduce the energy production by 10%, so ELF=0.90. This is a reasonable value for a site that does not experience heavy icing.
4. The sample uncertainty values of the long-term hub height Weibull parameters, the power production, and the ELF are given in Table 1. These values are meant to be representative of typical values for the uncertainty of the parameters and are not based on an actual site.

The result of the sample calculation is a value for CF=38.0%. This is calculated using Eq. (24) and a numerical integration program. The values for the sensitivity factors for c and k are $SF_{CF,c}=1.85$ and $SF_{CF,k}=0.07$. Using the sensitivity factors and the sample uncertainties, the overall CF uncertainty δCF is 17.2%. To obtain the absolute standard uncertainty, δCF is multiplied by CF, yielding a value of 0.06. Thus, the estimate of CF is $CF = 0.38 \pm 0.06$.

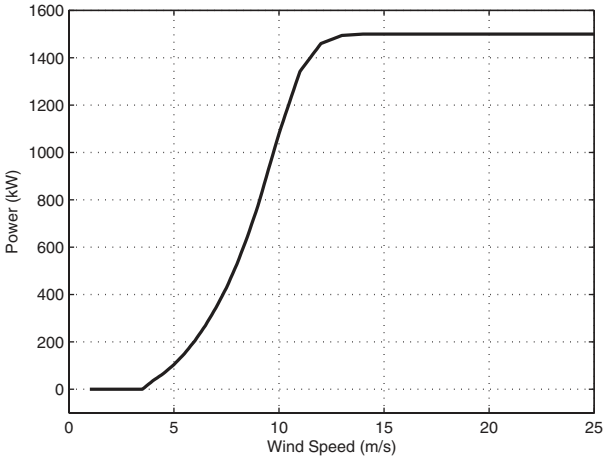

Fig. 3 Sample power curve

6.4 Example Calculation Discussion. The value of CF is dependent on the values of both c and k. This dependency is illustrated in Fig. 4, which shows the value of CF for ranges of values of c and k using the same power curve and ELF value as the example. Figure 4 clearly shows that CF increases as c increases. This comes as no surprise, as the value of c is directly proportional to the mean wind speed. Also, CF tends to increase as k increases, except when c is very small. As k increases, the Weibull distribution becomes less spread out and therefore more concentrated about its expected value. At very low values of c, this means that the distribution is concentrated about very low values of the wind speed, and so the turbine produces very little power, even when it is above the cut-in wind speed. However, for moderate to high values of c, a high k value results in the wind speed being above the cut-in value for a very high percentage of the time and, therefore, a high CF.

Table 1 Sample uncertainty values

δc	δk	δP	δELF
8%	8%	8%	4.0%

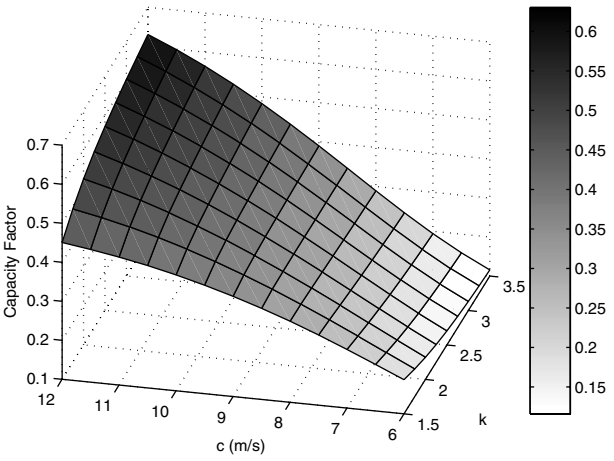

Fig. 4 Dependence of CF on *c* and *k*

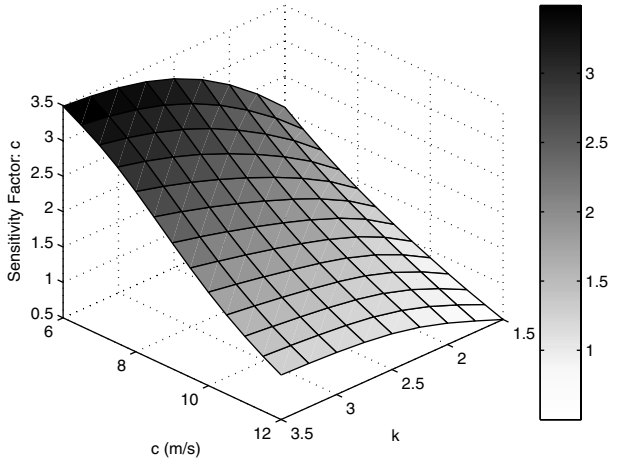

Fig. 5 Dependence of $SF_{CF,c}$ on *c* and *k*

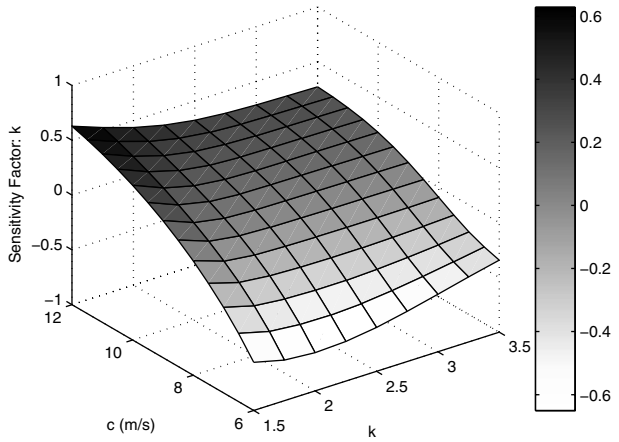

Fig. 6 Dependence of $SF_{CF,k}$ on *c* and *k*

The magnitude of δCF depends predominantly on the value of δc. In fact, if δk, δP, and δ ELF are all 0%, the uncertainty in CF is still 14.8%. This is due to the large magnitude of $SF_{CF,c}$. Thus, reducing δc (or mean wind speed) provides the best opportunity for reducing the overall CF uncertainty.

$SF_{CF,c}$ is 1.85. This is lower than is generally assumed. It is common practice to assume that a percentage increase in *c* (or the mean wind speed) causes between two and three times the percentage increase in CF, i.e., a sensitivity factor between 2 and 3 [1]. This is an oversimplification, however; and the results indicate that this assumption could lead to large errors. For example, if one had assumed that $SF_{CF,c}=2.3$, then δCF would be 20.5% instead of 17.2%. This could mean the difference between an acceptable and unacceptable risk level for a potential wind energy venture. In general, the values of the sensitivity factors should be calculated explicitly and not assumed.

In reality, $SF_{CF,c}$ is highly dependent on the value of *c*. $SF_{CF,c}$ decreases as *c* increases, and it increases as *k* increases. The dependence of $SF_{CF,c}$ on *c* and *k* for this example is shown in Fig. 5. The plot indicates that $SF_{CF,c}$ approximately decreases proportionally to the square of *c*. As *c* increases, the wind speed is above the rated wind speed more and more frequently. Therefore, any error in the estimation of *c* affects the value of CF less since the turbine produces constant power the above rated wind speed regardless of the actual wind speed. As *k* increases, the Weibull distribution becomes less spread out, resulting in the wind speed being close to the mean value more frequently. For a given value of *c*, a higher value of *k* results in the wind speed being less than the rated wind speed more often, and therefore the CF is more dependent on the value of *c*; hence $SF_{CF,c}$ is larger.

In this example, $SF_{CF,k}$ is fairly small relative to the other sensitivity factors, indicating that CF has a weak dependence on *k*. For example, a 10% increase in *k* would only change CF by 0.7%. However, $SF_{CF,k}$ is also highly dependent on the value of both *c* and *k*, as shown in Fig. 6, and so in some cases, uncertainty in *k* could contribute significantly to the overall uncertainty.

The value of *k* is often assumed to be approximately 2, although it can vary widely, with values that may be as low as 1.5 or as high as 3.5 at some sites. The value of *k* is not insignificant. For this example, if one assumes that *k* is equal to 2 but is in fact, equal to 1.5, the CF would be calculated as 0.374 or 0.357, respectively. This may seem like a small difference, but it corresponds to a 5% change in AEP, which can make the difference between a successful venture and a failure. Thus, assuming a value of *k* may have adverse consequences because it could lead to an incorrect estimation of CF (or AEP). This further reinforces the utility of using the two parameter Weibull distribution to approximate the wind speed distribution rather than the one parameter Rayleigh distribution.

7 Recommendations

The sample calculation above demonstrates that uncertainty in *c* is typically the dominant contributor to δCF. Thus, reducing δc is the logical starting point when attempting to reduce the overall uncertainty in site assessment. Wind measurement devices capable of measuring at hub height offer one approach to accomplish this goal. These devices, such as a LIDAR, SODAR, eliminate errors due to shear model uncertainty and tower/boom effects [34,35]. Also, the measurement uncertainty sensitivity factor is one when measuring at hub height, which further reduces the wind resource uncertainty. In fact, a LIDAR or SODAR with 5% measurement uncertainty would reduce the uncertainty in CF to 12.9% from 17.2%, which is a decrease in the uncertainty of approximately 25%. Tall towers can also be used for hub height measurements. With all of these alternative options, cost and reliability are mitigating factors that must be balanced against the potential reduction in uncertainty. Nonetheless, these results suggest that serious consideration should be given to these alternative measurement methods as effective means of reducing the uncertainty in the site assessment process.

8 Conclusion

Wind energy site assessment is a complex multistep process, with a high degree of uncertainty. This paper seeks to present a framework for handling uncertainties in a common approach to this process when met towers are used to measure the wind resource, and MCP is used to estimate the long-term wind resource. Mathematically rigorous methods for estimating uncertainty are presented. These methods utilize sensitivity factors to combine independent sources of uncertainty. Specifically, the wind speed measurement uncertainty sensitivity factor and the Weibull parameter sensitivity factors can be calculated explicitly using the methods outlined in this paper. This eliminates the need to assume the values for sensitivity factors or ignore them altogether. The result is that the uncertainty in the site assessment process can be calculated more accurately.

Acknowledgment

The authors would like to acknowledge the support of the Massachusetts Technology Collaborative for their support of the research on which this paper is based.

Nomenclature

array = denotes array losses
av = denotes availability losses
c = Weibull scale factor
foul = denotes fouling losses
k = Weibull shape factor
h = height
hub = denotes hub height quantities
LT = denotes long-term quantities or long-term estimation uncertainty
LT_hub = denotes long-term hub height quantities
M = denotes measured quantities or measurement uncertainty
N = number of measurements
P = power
P_R = rated wind turbine power
$P_W(U)$ = wind turbine power curve
P_W = average power output
$p(U)$ = wind speed probability density function
R = range of a rectangular distribution
SA = denotes site assessment uncertainty
SF = sensitivity factor
U = wind speed
$\bar{U}$ = mean wind speed
V = denotes interannual variability uncertainty
z_0 = log law wind shear parameter
α = power law wind shear parameter
Γ = gamma function
Ψ = psi function
δ = denotes uncertainty
σ = standard deviation
$*$ = denotes absolute uncertainties (versus nondimensional uncertainties)

References

[1] Frandsen, S., and Christensen, C. J., 1992, "Accuracy of Estimation of Energy Production From Wind Power Plants," Wind Eng., **16**(5), pp. 257–268.
[2] Pedersen, T. F., 2004, "Power Curve Measurements Under Influence of Skew Airflow and Turbulence," Risø National Laboratory Report.
[3] Mortensen, N. G., 1994, "Wind Measurements for Wind Energy Applications: A Review," *British Wind Energy Association Conference*, Sirling, GB.
[4] Baily, B., 1997, "Wind Resource Assessment Handbook," AWS Scientific, Inc. Report.
[5] Quarton, D., 2004, "Wind Turbines—Part 121: Power Performance Measurements of Grid Connected Wind Turbines," IEC 61400-12, Ed. 1.
[6] Manwell, J. F., McGowan, J. G., and Rogers, A. L., 2002, *Wind Energy Explained*, Wiley, West Sussex, England, Chap. 2.
[7] Frandsen, S., 1991, "Uncertainty on Wind Turbine Power Curve Measurements," *British Wind Energy Association Conference*, Swansea, GB.
[8] Taylor, J., 1997, *An Introduction to Error Analysis*, 2nd ed., University Science Books, Sausalito, CA, Chaps. 1–4.
[9] Lockhart, T., and Bailey, B., 1998, "The Maximum Type 40 Anemometer Calibration Project," NRG Systems Report (available at http://www.nrgsystems.com/store/product_detail.php?cd=11&s=1899&tab=support.
[10] Pedersen, T. F., 2004, "Characterisation and Classification of RISØ P2546 Cup Anemometer," Risø National Laboratory Report.
[11] Kristensen, L., 1999, "The Perennial Cup Anemometer," Wind Energy, **2**, pp. 59–75.
[12] Papadopoulos, K. H., Stefanatos, N. C., Paulsen, U. S., and Morfiadakis, E., 2001, "Effects of Turbulence and Flow Inclination on the Performance of Cup Anemometers in the Field," Boundary-Layer Meteorol., **101**, pp. 77–107.
[13] Albers, A., Klug, H., and Westermann, D., 2000, "Outdoor Comparisons of Cup Anemometers," DEWI Magazine, **17**, pp. 5–15.
[14] Kline, J., 2002, "Effects of Tubular Anemometer Towers on Wind Speed Measurements," *AWEA Windpower 2002*, Portland, OR.
[15] Maribo Pedersen, B., Hansen, K. S., Oye, S., Brinch, M., and Fabian, O., 1992, "Some Experimental Investigations on the Influence of the Mounting Arrangements on the Accuracy of Cup-Anemometer Measurements," J. Wind. Eng. Ind. Aerodyn., **39**, pp. 373–383.
[16] Baker, R. W., Walker, S. N., and Wade, J. E., 1990, "Annual and Seasonal Variations in Mean Wind Speed and Wind Turbine Energy Production," Sol. Energy, **45**(5), pp. 285–289.
[17] Klink, K., 2002, "Trends and Interannual Variability of Wind Speed Distributions in Minnesota," J. Clim., **15**, pp. 3311–3317.
[18] Landberg, L., and Mortensen, N. G., 1993, "A Comparison of Physical and Statistical Methods for Estimating the Wind Resource at a Site," *British Wind Energy Association Conference*, York, GB.
[19] Landberg, L., Myllerup, L., Rathman, O., Petersen, E. L., Jørgensen, B. H., Badger, J., and Mortensen, N. G., 2003, "Wind Resource Estimation: An Overview," Wind Energy, **6**(3), pp. 261–271.
[20] Rogers, A. L., Rogers, J. W., and Manwell, J. F., 2005, "Uncertainties in Results of Measure-Correlate-Predict Analyses," *AWEA Windpower 2005*, Denver, CO.
[21] Breslow, P. B., and Sailor, D. J., 2002, "Vulnerability of Wind Power Resources to Climate Change in the Continental United States," Renewable Energy, **27**, pp. 585–598.
[22] Elkinton, M. R., Rogers, A. L., and McGowan, J. G., 2006, "An Investigation of Wind-Shear Models and Experimental Data Trends for Different Terrains," Wind Eng., **30**(4), pp. 341—350.
[23] Livingston, J. T., and Anderson, T., 2004, "Wind Shear, Taller Turbines, and the Effects on Wind Farm Development Create a Need for Taller MET Towers," Windtower Composites Report (http://compositetower.com/pdf/windshearpositiondoc.pdf).
[24] Brower, M., 2006, "The Role of Wind Flow Modeling and Mapping," *AWEA and CanWEA Resource Assessment Workshop*, Syracuse, NY.
[25] Doran, J. C., and Verholek, M. G., 1977, "A Note on Vertical Extrapolation Formulas for Weibull Velocity Distribution Parameters," J. Appl. Meteorol., **17**(3), pp. 410–412.
[26] Wieringa, J., 1989, "Shapes of Annual Frequency Distributions of Wind Speed Observed on High Meteorological Masts," Boundary-Layer Meteorol., **47**, pp. 85–110.
[27] Rogers, A. L., Rogers, J. W., and Manwell, J. F., 2005, "Comparison of the Performance of Four Measure-Correlate-Predict Algorithms," J. Wind. Eng. Ind. Aerodyn., **93**(3), pp. 243–264.
[28] Taylor, M., Machiewicz, P., Brower, M., and Markus, M., 2005, "Quantifying Uncertainty in Wind Resource Estimates," *AWEA Windpower 2005*, Denver, CO.
[29] Pedersen, T. F., Gjerding, S., Ingham, P., Enevoldsen, P., Hansen, J. K., and Jørgensen, H. K., 2002, "Wind Turbine Power Performance Verification in Complex Terrain and Wind Farms," Risø National Laboratory Report.
[30] Jones, S., 2006, "Examining Project Underperformance," *AWEA Windpower 2006*, Pittsburgh, PA.
[31] Homola, M. C., 2005, "Impacts and Causes of Icing on Wind Turbines," Navrik University College Report.
[32] Bailey, B., and Brower, M., 2004, "Estimation of the Long-Term Average Wind Speed and Energy Production at the Proposed East Mountain Wind Project Site," AWS True Wind, LLC Report.
[33] Jensen, N. O., 1983, "A Note on Wind Generator Interaction," Risø National Laboratory, Report No. Risø-M-2411.
[34] Smith, D. A., Harris, M., Coffey, A. S., Mikkelsen, T., Jørgensen, H. E., Mann, J., and Danielian, R., 2006, "Wind LIDAR Evaluation at the Danish Wind Test Site in Horsore," Wind Energy, **9**, pp. 97–93.
[35] Rogers, A. L., Walls, E., Henson, W., and Manwell, J. F., 2007, "Addressing Ground Clutter Corruption of Sodar Measurements," *45th AIAA Aerospace Sciences Meeting and Exhibit (ASME Wind Energy Symposium)*, Reno, NV.